

Diastereoselective Reactions in Glycine Templates Containing an *ent*-Ardeemin Fragment

Sonsoles Martín-Santamaría,^{†,‡,§} Raúl Corzo-Suárez,^{||} Carmen Avendaño,^{*,‡} Modesta Espada,[‡] Federico Gago,[§] Santiago García-Granda,^{||} and Henry S. Rzepa[†]

Department of Chemistry, Imperial College of Science, Technology and Medicine, London SW7 2AY, United Kingdom, Departamento de Química Orgánica y Farmacéutica, Facultad de Farmacia, Universidad Complutense, 28040 Madrid, Spain, Departamento de Química Física y Analítica, Facultad de Química, Universidad de Oviedo, 33006 Oviedo, Spain, and Departamento de Farmacología, Universidad de Alcalá, 28871 Alcalá de Henares, Madrid, Spain

avendano@farm.ucm.es

Received April 27, 2001

Self-consistent reaction field solvation models derived from SCF-MO calculations are shown to be reliable in modeling the diastereoselectivity of the reactions of the anion and cation derived from (4*S*)-2,4-dimethyl-2,4-dihydro-1*H*-pyrazino[2,1-*b*]quinazoline-3,6-dione (**1**) at C(1) with electrophiles and nucleophiles, respectively. The found anti/syn ratio of compound **8**, which is a *seco-ent*-ardeemin analogue obtained by alkylation of **1** with gramine methiodide, confirms this computational model. A close similarity between the calculated geometry of the piperazine ring in the anti isomers of 1,2,4-trialkyl derivatives and that deduced from their ¹H NMR (solution) and X-ray data has been also established.

Introduction

The fungal metabolite *N*-acetylardeemin (Figure 1) has been described as a potent inhibitor of multiple drug resistance (MDR) to antitumor agents.¹ We have previously reported the preparation of a wide range of simplified analogues containing rings D–F of ardeemin² by starting from (4*S*)-2,4-dialkyl derivatives such as **1**. This chemistry has shown that compounds related to **1** can be considered as nucleophilic or electrophilic glycine templates and that some tricyclic compounds retain most of the MDR-reversal activity of the prototype, mainly the 1,1,2-tribenzyl-4-methyl derivative.³

Alkylation of **1**, acting as a nucleophile glycine template, is a regio- and diastereoselective process in which the 1,4-anti isomers (Scheme 1) are preferent under kinetic conditions in all studied alkyl halides except for R = H and R = *p*-NO₂C₆H₄.^{2a} We rationalized that this stereochemistry arises from the asymmetric induction of

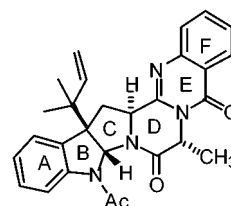


Figure 1. *N*-Acetylardeemin.

the C(4)-methyl group, which is locked in the starting material in a pseudoaxial disposition in order to avoid the steric interaction with the nearly coplanar C(6)-carbonyl group.⁴ The observed equilibration of the anti isomers to the syn isomers under thermodynamic conditions was supposed to minimize the interaction between the alkyl substituents at C(1) and at N(2).

However, inter- and intramolecular additions of nucleophiles to *N*-acyliminium cations derived from 1-tosyloxy,^{2f} 1-hydroxy,^{2h} 1-alkoxy,^{2f,2h} and 1-bromo²ⁱ derivatives of the (4*S*)-2-alkyl-4-methyl system showed that these compounds behave as electrophilic glycine templates to give diastereoselectively the corresponding syn isomers (see compounds **6** and **7** in Scheme 2), without traces of the anti isomers in nearly all intermolecular reactions.

To explain this peculiar stereoselection, we have conducted a theoretical study on compounds **2–7** by applying several methodologies. We have also prepared compound **8**, which is a *seco-ent*-ardeemin analogue to confirm the computational model and, finally, we have studied by X-ray diffraction analysis the structure of the anti isomer of **3**, to investigate whether the conformation of the piperazine ring deduced by MM calculations and from ¹H NMR data^{2a} is retained in the solid state.

[†] Imperial College of Science, Technology and Medicine.

[‡] Universidad Complutense.

[§] Universidad de Alcalá.

^{||} Universidad de Oviedo.

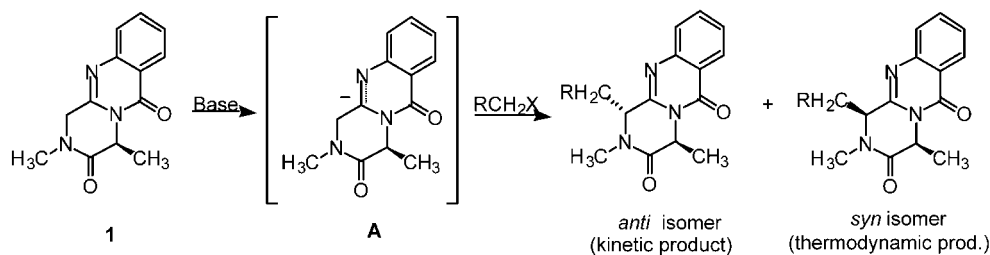
(1) (a) Karwoski, J. P.; Jackson, M.; Rasmussen, R. R.; Humphrey, P. E.; Poddig, J. B.; Kohl, W. L.; Kadam, S.; McAlpine, J. B. *J. Antibiot.* **1993**, *46*, 374. (b) You, M.; Wickramaratne, D. B. M.; Silva, G. L.; Chai, H.; Chagwedera, T. E.; Farnsworth, N. R.; Cordell, G. A.; Kinghorn, A. D.; Pezzuto, J. M. *J. Nat. Prod.* **1995**, *58*, 598.

(2) (a) Martín-Santamaría, S.; Buenadicha, F. L.; Espada, M.; Söllhuber, M.; Avendaño, C. *J. Org. Chem.* **1997**, *53*, 6425. (b) Martín-Santamaría, S.; Espada, M.; Avendaño, C. *Tetrahedron* **1997**, *53*, 16795. (c) Bartolomé, M. T.; Buenadicha, F. L.; Avendaño, C.; Söllhuber, M. *Tetrahedron: Asymmetry* **1998**, *9*, 249. (d) Buenadicha, F. L.; Avendaño, C.; Söllhuber, M. *Tetrahedron: Asymmetry* **1998**, *9*, 4275. (e) Fernández, M.; Heredia, M. L.; de la Cuesta, E.; Avendaño, C. *Tetrahedron* **1998**, *54*, 2777. (f) Martín-Santamaría, S.; Espada, M.; Avendaño, C. *Tetrahedron* **1999**, *55*, 1755. (g) Buenadicha, F. L.; Bartolomé, M. T.; Aguirre, M. J.; Avendaño, C.; Söllhuber, M. *Tetrahedron: Asymmetry* **1998**, *9*, 483. (h) Sánchez, J. D.; Ramos, M. T.; Avendaño, C. *Tetrahedron Lett.* **2000**, *41*, 2745. (i) Heredia, M. L.; de la Cuesta, E.; Avendaño, C. *Tetrahedron: Asymmetry* **2001**, *12*, 411. (j) Heredia, M. L.; de la Cuesta, E.; Avendaño, C. *Tetrahedron* **2001**, *57*, 1987.

(3) Méndez-Vidal, C.; Rodríguez, A. *Cancer Lett.* **1998**, *132*, 45.

(4) (a) Rajappa, S.; Advani, B. G. *J. Chem. Soc., Perkin Trans. 1* **1974**, 2122. (b) Suguna, K.; Ramakumar, S.; Rajappa, S. *Acta Crystallogr. B* **1995**, *B38*, 1654.

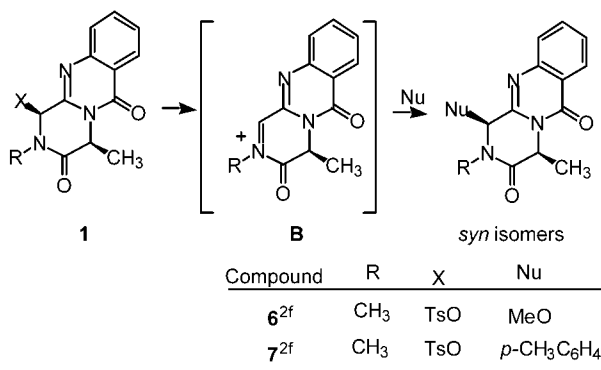
Scheme 1



Compound	R ^a
2	H
3	C ₆ H ₅
4	<i>p</i> -NO ₂ C ₆ H ₄
5	<i>p</i> -FC ₆ H ₄

^aOther R groups studied in Ref. 2a were:
CH=CH₂, *p*-CH₃C₆H₄, *m*-ClC₆H₄, *o*-FC₆H₄,
p-CF₃C₆H₄, 2-naphthyl.

Scheme 2



Results and Discussion

Computational Modeling. We started by modeling the transition states corresponding to the alkylation of anion A and selected four electrophiles: benzyl bromide, *p*-fluorophenylmethyl bromide, methyl iodide, and *p*-nitrophenylmethyl bromide. Benzyl bromide^{2a} and *p*-fluorophenylmethyl bromide^{2a} were typical in giving the anti isomers as the major products under kinetic control conditions (compounds 3 and 5, Scheme 1). Other halides that gave similar experimental results were allyl, *p*-methylphenylmethyl, 2-naphthylmethyl, *m*-chlorophenylmethyl, *o*-fluorophenylmethyl, and *p*-trifluoromethylphenylmethyl halides. On the contrary, methyl iodide and *p*-nitrophenylmethyl bromide were unusual in giving the syn isomers (compounds 2 and 4) as single or major products, respectively, under identical conditions (−78 °C, 20 min).^{2a}

In view of the involvement of ionic intermediates, we felt it imperative to characterize the potential energy surfaces not only in the gas phase but also with a continuum model⁵ representing the tetrahydrofuran solvent employed. Although lithiated species are known to exist mostly as contact ion pairs, anion A was used as reaction intermediate in the model because the employment of bases different to LHMDS, for instance KHMDS, gave identical diastereoselectivity.

After an initial semiempirical study using PM3 parameter set⁶ and the COSMO solvation model, we

performed ab initio calculations using the 3-21G(d) basis set⁷ at the Hartree–Fock (HF) and B3LYP density functional levels in the gas phase and in the Tomasi continuum model (PCM).

The computed geometry for anion A showed a planar disposition for the piperazine ring, being the HOMO molecular orbital mainly localized at C(1) with minor coefficients at N(11) and at the fused benzene ring. Transition-state geometries and significant distances corresponding to the reaction of anion A with benzyl bromide are shown in Figure 2.

The semiempirical level calculations predicted that the activation barriers for the syn-attack transition state are lower in all cases, without important differences between gas phase and solvated PM3 models (Table 1, entries 1, 2, 7, 8, 13, 14, 19, and 20). However, the results from the ab initio Tomasi solvation model at the HF and B3LYP density functional levels were in accordance with an anti attack for benzyl and *p*-fluorophenylmethyl bromides (Table 1, compounds 3 and 5, entries 10, 22 (HF) and 12, 24 (B3LYP), respectively), as was shown by their lower activation barriers, and with a syn attack for methyl iodide and *p*-nitrophenylmethyl bromide (Table 1, compounds 2 and 4, entries 4, 16 (HF) and 6, 18 (B3LYP), respectively).

Therefore, this method appeared to be more appropriated for reproducing the experimental kinetic conditions although the low differences between both, the energies of the transition states and the activation barriers in the reaction with methyl iodide do not explain the absence of any anti isomer of 2. This experimental result may be a consequence of the easy epimerization of this compound,^{8,9} a fact that can be rationalized taking into account that the lower steric interactions between the (C1) and N(2) substituents in the anti isomers of 1-methyl derivatives of this tricyclic system permit a conformation of the piperazine ring that places the C(1)–H bond parallel to the *p* orbitals of the C(11a)–N(11) double bond under the reaction conditions. It is also possible that the greater acidity of H-1 in compound 4 promotes the epimerization of the anti to the syn isomer.

(7) The employment of larger basis sets that would include bromine and iodine (as external double or triple zeta basis sets) was precluded because of the size of the systems.

(8) Wang, H.; Ganesan, A. *J. Org. Chem.* **2000**, *65*, 1022.

(9) Buenadicha, F. L.; Avendaño, C.; Söllhuber, M. *Tetrahedron: Asymmetry* **2001**, *12*, 3019.

(5) Barone, V.; Cossi, M.; Tomasi, J. *Comput. Chem.* **1998**, *19*, 404.
(6) AM1 geometries did not converge.

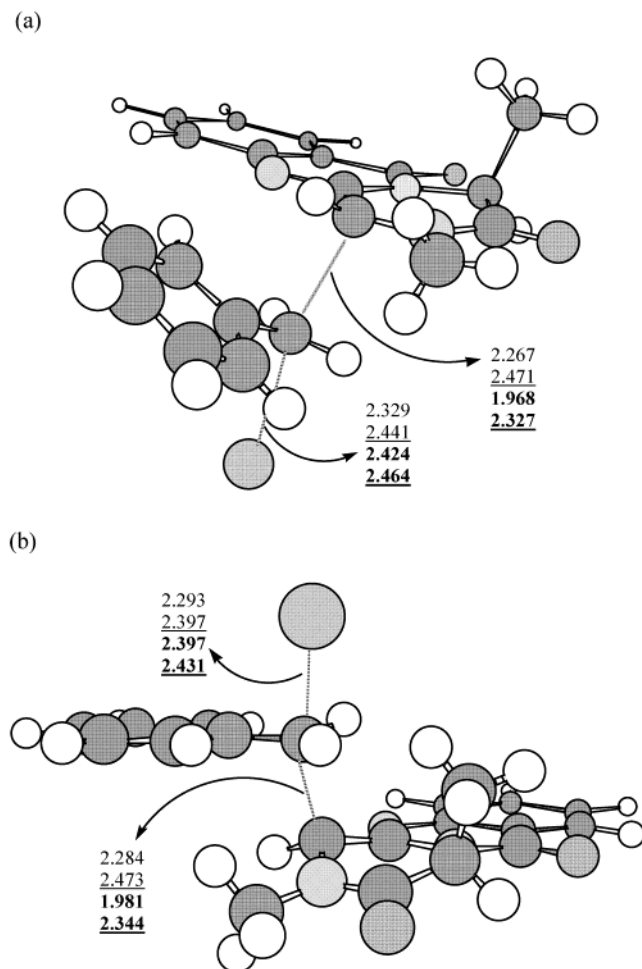


Figure 2. Calculated [PM3, RHF/3-21G(d); gas phase versus solvated models] significant distances (Å) in the transition structures for anti (a) and syn attack (b) of benzyl bromide on anion **A**.

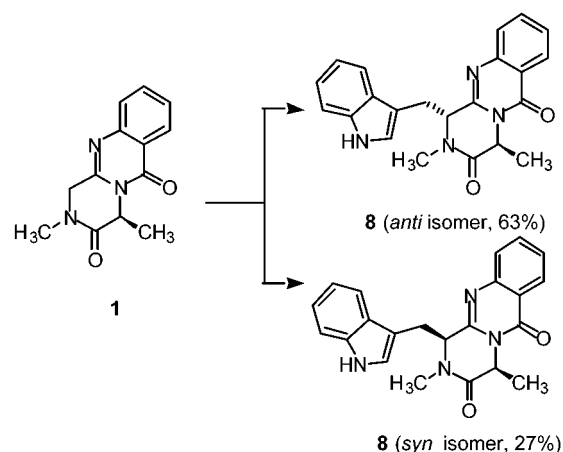
Our model was extended to the alkylation of **1** with gramine methiodide¹⁰ to test the reliability of the method for predicting the diastereoselectivity of this reaction and to obtain compounds **8**, which are *seco* analogues of *ent*-ardeemin, by a procedure that is an alternative to other previously described.¹¹ The ab initio Tomasi solvation model (Table 1, entries 28 and 30) showed lower activation barriers for the anti attack, suggesting the 1,4-anti isomer of **8** as the main product under kinetic conditions. The experimental evidence was consistent with the theoretical prediction, since we obtained a global alkylation yield of 90% with a diastereomeric ratio of 3:1 in favor of the anti isomer (Scheme 3). Both isomers showed ee >95% according to ¹H NMR experiments by using chiral reagents and by comparing to a racemic sample.

We continued by modeling the nucleophilic attack of the intermediate cation **B**, whose computed geometry also showed a planar disposition. The shortened C(1)–N(2) bond (1.316 Å at the semiempirical level) indicates the presence of a strong electron donating effect from the N(2) on the C(1) position, which is typical for an iminium cation. The LUMO was mainly located at C(1) with a

Table 1. Activation Barriers (kcal mol⁻¹) for the Stationary Point Structures (the Solvent is THF)

entry	method	activation barrier anti/syn	exptl anti/syn ratio	calcd anti/syn ratio
2 , R = H, X = I				
1	PM3, gas phase	9.3/6.3	0/100	37/63
2	PM3, COSMO	14.6/12.0		1/99
3	RHF/3-21G(d), gas phase	5.4/4.7		23/77
4	RHF/3-21G(d), PCM	9.1/8.5		27/73
5	B3LYP/3-21G(d), gas phase	3.3/2.4		18/82
6	B3LYP/3-21G(d), PCM	9.7/5.7		0.1/99.9
3 , R = Ph, X = Br				
7	PM3, gas phase	13.5/10.9	87/13	1/99
8	PM3, COSMO	14.8/14.3		30/70
9	RHF/3-21G(d), gas phase	12.2/10.6		6/94
10	RHF/3-21G(d), PCM	11.7/21.0		99.99/0.01
11	B3LYP/3-21G(d), gas phase	6.3/4.7		6/94
12	B3LYP/3-21G(d), PCM	9.6/18.1		99.99/0.01
4 , R = <i>p</i> -NO ₂ -Ph, X = Br				
13	PM3, gas phase	5.9/3.7	10/90	2/98
14	PM3, COSMO	15.5/13.5		3/97
15	RHF/3-21G(d), gas phase	4.3/2.9		9/91
16	RHF/3-21G(d), PCM	10.5/9.6		18/82
17	B3LYP/3-21G(d), gas phase	3.3/2.0		10/90
18	B3LYP/3-21G(d), PCM	6.5/5.3		13/87
5 , R = <i>p</i> -F-Ph, X = Br				
19	PM3, gas phase	11.1/8.4	71/29	1/99
20	PM3, COSMO	14.5/12.5		3/97
21	RHF/3-21G(d), gas phase	9.6/8.0		6/94
22	RHF/3-21G(d), PCM	11.2/12.8		94/6
23	B3LYP/3-21G(d), gas phase	4.1/2.7		9/91
24	B3LYP/3-21G(d), PCM	9.1/10.0		82/18
8 , R = 3-indolylmethyl, X = Br				
25	PM3, gas phase	15.1/15.5	70/30	66/34
26	PM3, COSMO	18.1/16.1		3/97
27	RHF/3-21G(d), gas phase	12.3/10.4		4/96
28	RHF/3-21G(d), PCM	13.9/14.7		79/21
29	B3LYP/3-21G(d), gas phase	3.8/1.5		2/98
30	B3LYP/3-21G(d), PCM	7.9/9.9		97/3

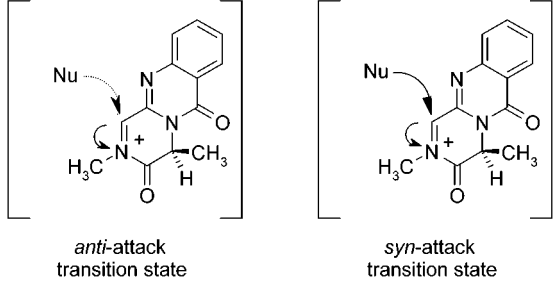
Scheme 3



minor coefficient at N(2). To study the stereoselectivity of the nucleophilic attack on this cation, we proceeded to model the transition states in which either methanol or toluene acted as nucleophiles to give compounds **6** or **7**, respectively.^{2f} For nucleophilic attack of toluene, the semiempirical (Table 2, entries 6 and 7) and ab initio methods (Table 2, entries 8–10), both in the gas phase and by using solvated models, correctly predicted the

(10) (a) Geissman, T. A.; Armen, A. *J. Am. Chem. Soc.* **1952**, *74*, 3916. (b) 3-Indolylmethyl bromide was used in order to simplify the calculations.

(11) Caballero, E.; Avendaño, C.; Menéndez, J. C.; *Heterocycles* **2000**, *53*, 1765.

Table 2. Activation Barriers (kcal mol⁻¹) for the Stationary Point Structures (the Solvent Is Methanol for **6** and Toluene for **7**)


entry	method	activation barrier		calcd anti/syn ratio
		anti/syn	exptl anti/syn ratio	
6 , Nu = MeOH				
1	PM3, gas phase ^a	19.1/18.0	0/100	14/86
2	RHF/3-21G(d), gas phase	18.4/15.7		1/99
3	RHF/3-21G(d), PCM	18.9/16.0		1/99
4	B3LYP/3-21G(d), gas phase	13.3/3.3		0.01/99.99
5	B3LYP/3-21G(d), PCM	16.0/11.1		0.01/99.99
7 , Nu = Toluene				
6	AM1, gas phase	10.9/9.5	0/100	9/91
7	AM1, COSMO	12.2/10.7		7/93
8	RHF/3-21G(d), gas phase	10.5/8.3		2/98
9	RHF/3-21G(d), PCM	11.4/10.0		9/91
10	B3LYP/3-21G(d), gas phase ^b	7.4/5.4		3/97

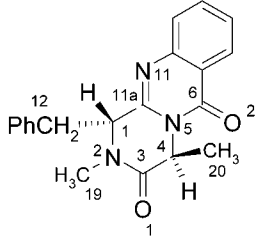
^a Geometry not locatable with COSMO model. ^b Geometry not locatable with PCM.

transition structures for the syn attack to be the most stable to give compounds **7**. This transition state corresponds to an aromatic S_E reaction as it is shown in Figure 3. The most stable transition state for the syn attack corresponds to a conformation where the aromatic ring adopts an exo configuration. In contrast, this ring adopts an endo configuration in the anti transition state, facing the piperazine ring (the alternate exo conformation was 0.4 kcal mol⁻¹ less stable than the endo).

The syn attack of methanol to give compound **6** has also lower calculated activation energies (Table 2, entries 1–5).

We conclude that self-consistent reaction field solvation models derived from ab initio SCF-MO calculations are reliable in modeling the diastereoselectivity of the reaction of the anion and cation derived from **1** at C(1) with electrophiles and nucleophiles, respectively. The presence of the metal cation is an important factor for the anti selectivity in the alkylation reactions.

X-ray Crystal Structure of 3 (1,4-Anti Isomer). This analysis was performed in order to investigate if the quasi-planar conformation of the piperazine ring which was shown by the 1,4-anti isomers of this system in solution is retained in the solid state. We have already reported that molecular mechanics (MM) calculations confirmed the greater stability of the syn isomers of compounds **2–5** over the anti isomers,^{2a} being the calculated MM geometries in complete agreement with NMR data. These studies showed that the piperazine ring in the syn isomers adopts a boat conformation with the N(2)-methyl group pseudoequatorial, being the C(4)-methyl and the C(1)-substituent in a pseudoaxial disposition. In contrast, the piperazine ring in the anti isomers is in a planar chair conformation, which implies greater steric interactions between the C(1)-substituents and the

Table 3. Values for Some of the Torsion Angles of **3** (1,4-Anti Isomer)


torsion angle	degrees (standard deviation)
O1–C3–C4–N5	–175.9 (6)
N11–C11a–C1–N2	156.0 (7)
N2–C3–C4–N5	0.0 (1)
C11a–N5–C4–C3	4.5 (9)
C19–N2–C3–C4	–176.0 (7)
O1–C3–C4–C20	–54.1 (9)

pseudoequatorial N(2)-methyl group. The X-ray diffraction studies confirmed the planar geometry of **3** (1,4-anti isomer) as it is shown in the crystallographic data of Table 3, where representative dihedral angles are close to 0° or 180°, except those including C(1) or C(4) substituents.

Experimental Section

Computational Procedure. Geometries of all species were initially defined using the MacMolPlt program.¹² All putative saddle points were characterized by calculation of the force constant matrix and normal coordinate analysis and in selected cases by computing an intrinsic reaction coordinate calculation along the first normal mode direction to verify the identity of the reactant and products deriving from the transition state. Calculations at the SCRf-RHF and B3LYP levels were performed using the Gaussian 98 program system¹³ and at the semiempirical SCRf-SCF-MO level using the MOPAC2000 program.¹⁴ Activation barriers correspond to the relative energies between transition states and their corresponding starting materials. Energies and first normal mode for the stationary point structures are collected in Tables 4 and 5 (see the Supporting Information).

X-ray Experimental Data. Data were collected on a Nonius CAD4 single-crystal diffractometer. The intensities were measured using the ω - 2θ scan technique with a scan angle of 1.5° and a variable scan rate with a maximum scan time of 60 s per reflection. The intensity of the primary beam was checked throughout the collection by monitoring three standard reflections every 60 min. On all reflections, profile analysis was performed.¹⁵ Symmetry-equivalent reflections were averaged and Lorentz and polarization corrections were

(12) Bode, B. M.; Gordon, M. S. *J. Mol. Graphics Mod.* **1998**, 133.

(13) Gaussian 98 (Revision A.1): Frisch, M. J.; Trucks, G. W.; Schlegel, H. B.; Scuseria, G. E.; Robb, M. A.; Cheeseman, J. R.; Zakrzewski, V. G.; Montgomery, J. A.; Stratmann, R. E.; Burant, J. C.; Dapprich, S.; Millam, J. M.; Daniels, A. D.; Kudin, K. N.; Strain, M. C.; Farkas, O.; Tomasi, J.; Barone, V.; Cossi, M.; Cammi, R.; Mennucci, B.; Pomelli, C.; Adamo, C.; Clifford, S.; Ochterski, J.; Petersson, G. A.; Ayala, P. Y.; Cui, Q.; Morokuma, K.; Malick, D. K.; Rabuck, A. D.; Raghavachari, K.; Foresman, J. B.; Cioslowski, J.; Ortiz, J. V.; Stefanov, B. B.; Liu, G.; Liashenko, A.; Piskorz, P.; Komaromi, I.; Gomperts, R.; Martin, R. L.; Fox, D. J.; Keith, T.; Al-Laham, M. A.; Peng, C. Y.; Nanayakkara, A.; Gonzalez, C.; Challacombe, M.; Gill, P. M. W.; Johnson, B. G.; Chen, W.; Wong, M. W.; Andres, J. L.; Head-Gordon, M.; Replogle, E. S.; Pople, J. A. Gaussian, Inc., Pittsburgh, PA, 1998.

(14) MOPAC2000: Stewart, J. J. P. Fujitsu Limited, Tokyo, Japan, 1999.

(15) (a) Lehman, M. S.; Larsen, F. K. *Acta Crystallogr. A* **1974**, 30, 580. (b) Grant, D. F.; Gabe, E. J. *J. Appl. Crystallogr.* **1978**, 11, 114.

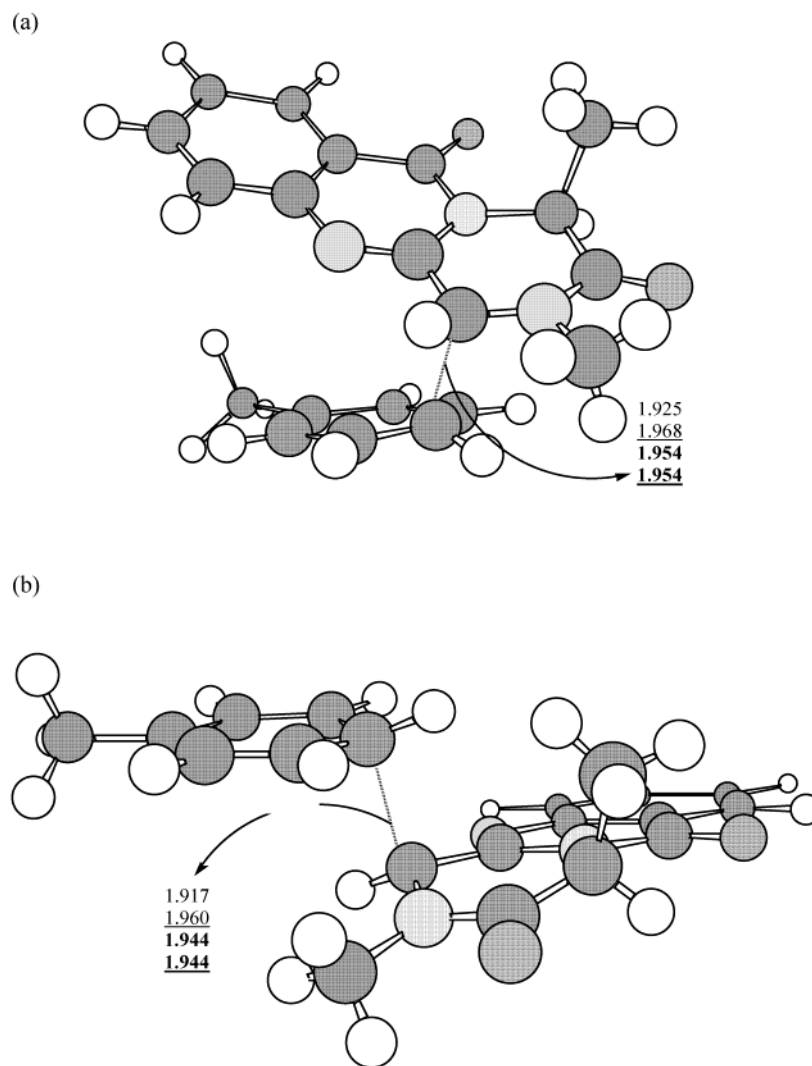


Figure 3. Calculated [AM1, RHF/3-21G(d); gas phase versus solvated models] significant distances (Å) in the transition structures for anti (a) and syn attack (b) of toluene on cation **B**.

applied. The structure was solved by direct methods using SHELXS97.¹⁶ Isotropic least-squares refinement on F^2 using SHELXL97.¹⁷ Empirical absorption correction was applied using XABS2.¹⁸ An extinction parameter x_{exti} was refined, so F_c is multiplied by $[k[1 + 0.001x_{\text{exti}}F_c^2\lambda^3/\sin(2\theta)]^{-1/4}]$. During the final stages of the refinements, all positional parameters and the anisotropic temperature factors of all the non-H atoms were refined. The H-atoms were geometrically calculated and refined with a common isotropic thermal parameter. The function minimized was $[\sum[w(F_o^2 - F_c^2)^2/\sum[w(F_o^2)^2]]^{1/2}]$ where $w = 1/[\sigma^2(F_o^2) + (0.0942P)^2 + 0.1470P]$ with $\sigma(F_o^2)$ from counting statistics and $P = (F_o^2 + 2F_c^2)/3$. Atomic scattering factors were taken from *International tables for X-ray Crystallography*.¹⁹ Plots were made with the EUCLID package.²⁰ Geometrical calculations were made with PARST.²¹ All calculations were made at the Scientific Computer Centre of the University of Oviedo and on the X-ray group computers.

(16) Sheldrick, G. M. SHELXS-97. *Program for the Solution of Crystal Structures*, University of Göttingen, 1997.

(17) Sheldrick, G. M. SHELXL-97. *Program for the Refinement of Crystal Structures*, University of Göttingen, 1997.

(18) Parkin, S.; Moezzi, B.; Hope, H. *J. Appl. Crystallogr.* **1995**, *28*, 53–56.

(19) *International Tables for X-ray Crystallography*, 1974; Birmingham, Kynoch Press: Birmingham, 1974 (present distributor: Kluwer Academic Publishers: Dordrecht); Vol. 4.

(20) Spek, A. L. In *Computational Crystallography*, Sayre, D., Ed.; Clarendon Press: Oxford, 1982; p 528.

(21) Nardelli, M. *Comput. Chem.* **1983**, *7*, 95.

The most relevant crystal and refinement data are collected in Tables 6–11 (see the Supporting Information). The unit-cell dimensions were determined from the angular settings of 25 reflections in the range $10 \leq \theta \leq 15^\circ$. The space group was inferred to be $P2_12_12_1$ from systematic absences. The absolute configuration was assigned based on the knowledge of that of the C(4) stereocenter.

Crystal data of compound 3. $M_r = 333.38$, orthorhombic, space group $P2_12_12_1$, $a = 8.309(7)$ Å, $b = 13.184(8)$ Å, $c = 15.993(5)$ Å, $V = 1751.9(19)$ Å³, $Z = 4$, $D_x = 1.264$ Mg/m³, Mo K α radiation (graphite crystal monochromator, $\lambda = 0.071073$ Å), $\mu = 0.083$ mm⁻¹, $F(000) = 704$, $T = 293(2)$ K. Final conventional $R = 0.0575$, $\omega R2 = 0.1389$ and $S = 1.018$, for 1779 “observed” reflections and 227 variables.

Chemical Procedures. Melting points are uncorrected. IR spectra were recorded with all solid compounds compressed into KBr pellets. NMR spectra were recorded at 250 MHz for ¹H and 62.5 MHz for ¹³C in CDCl₃, with TMS as the internal reference (Servicio RMN, UCM). Elemental analyses were obtained from the Servicio de Microanálisis, UCM. Optical rotations were determined at 25 °C in CHCl₃ or EtOH at 589 nm. Separations by flash chromatography were performed on silica gel (35–70 mm). Tetrahydrofuran was freshly distilled from sodium benzophenone. All reagents were commercial quality and were used as received. Starting material **1** was obtained according to the literature.^{4a}

Synthesis of Compounds 8. To a cold (–78 °C), magnetically stirred solution of compound **1** (1 mmol) in dry THF (15

mL) was added, under argon, dropwise via syringe a 1 M solution of lithium hexamethyl disilazide in THF (1 mL). After 5 min, this solution was added, via dry ice covered cannula, to a suspension of gramine methiodide (1.2 mmol) in dry THF (5 mL) at $-78\text{ }^{\circ}\text{C}$ under argon. The reaction mixture was maintained at $-78\text{ }^{\circ}\text{C}$ during 20 min, allowed to warm to room temperature, quenched with a cold saturated ammonium chloride solution (15 mL), and diluted with ethyl acetate. The separated aqueous layer was extracted with ethyl acetate ($3 \times 20\text{ mL}$) and the combined organic layers were washed, dried, and evaporated. Chromatography of the residue on silica gel (EtAcO/hexane, 1:1) provided first the anti isomer of **8** and next the syn isomer.

(1*R*,4*S*)-1-(3-Indolylmethyl)-2,4-dimethyl-2,4-dihydro-1*H*-pyrazino[2,1-*b*]quinazoline-3,6-dione (anti isomer of **8)** was obtained as a white solid: mp $178\text{--}180\text{ }^{\circ}\text{C}$; yield 63%; $[\alpha]_{\text{D}}^{25} +57$ (*c* 0.30, HCCl_3); IR $1685, 1658\text{ cm}^{-1}$; $^1\text{H NMR}$ (CDCl_3) δ 1.43 (d, 3H, $J = 6.7\text{ Hz}$, $\text{CH}_3\text{-4}$), 3.23 (s, 3H, CH_3N), 3.50 (dd, 1H, $J = 14.8, 3.6\text{ Hz}$, CH_2), 3.59 (dd, 1H, $J = 14.7, 3.0\text{ Hz}$, CH_2), 3.81 (q, 1H, $J = 6.7\text{ Hz}$, H-4), 4.95 (t, 1H, $J = 3.3\text{ Hz}$, H-1), 6.44 (t, 1H, $J = 7.1\text{ Hz}$, H-8), 6.59 (d, 1H, $J = 7.9\text{ Hz}$, H-7), 6.77 (d, 1H, $J = 2.4\text{ Hz}$, H-2'), 6.98 (t, 1H, $J = 7.1\text{ Hz}$, H-9), 7.23 (d, 1H, $J = 8.7\text{ Hz}$, H-10), 7.43 (ddd, 1H, $J = 7.5, 7.4, 1.4\text{ Hz}$, H-5'), 7.71 (d, 1H, $J = 7.6\text{ Hz}$, H-7'), 7.79 (ddd, 1H, $J = 7.6, 7.4, 1.5\text{ Hz}$, H-6'), 8.02 (dd, 1H, $J = 8.0, 1.2\text{ Hz}$, H-4'), 8.17 (wide s, 1H, NH); $^{13}\text{C NMR}$ (CDCl_3) δ 20.3 ($\text{CH}_3\text{-4}$), 30.3 (CH_2), 33.1 (CH_3N), 52.3 (C-4), 63.1 (C-1), 107.0 (C-3'), 111.4 (C-7'), 117.5 (C-4'), 119.8 (C-5'), 121.1 (C-6a), 122.5 (C-6'), 124.4 (C-2'), 126.6 (C-7), 126.7 (C-10), 126.8 (C-8), 126.9 (C-3a'), 134.6 (C-9), 135.8 (C-7a'), 146.9 (C-10a), 150.2 (C-11a), 159.9 (C-6), 168.4 (C-3). Anal. Calcd for $\text{C}_{22}\text{H}_{20}\text{N}_4\text{O}_2$: C, 70.97; H, 5.38; N, 15.05. Found: C, 71.02; H, 5.50; N, 15.06.

(1*S*,4*S*)-1-(3-indolylmethyl)-2,4-dimethyl-2,4-dihydro-1*H*-pyrazino[2,1-*b*]quinazoline-3,6-dione (syn isomer of **8)** was obtained as a white solid: mp $165\text{--}167\text{ }^{\circ}\text{C}$; yield 27%; $[\alpha]_{\text{D}}^{25} +19$ (*c* 0.20, HCCl_3); IR $1686, 1661\text{ cm}^{-1}$; $^1\text{H NMR}$ (CDCl_3) δ 1.05 (d, 3H, $J = 7.1\text{ Hz}$, $\text{CH}_3\text{-4}$), 2.90 (s, 3H, CH_3N), 3.55 (d, 2H, $J = 5.6\text{ Hz}$, CH_2), 4.85 (t, 1H, $J = 5.6\text{ Hz}$, H-1), 5.10 (q, 1H, $J = 7.1\text{ Hz}$, H-4), 6.93 (dd, 1H, $J = 7.9, 7.1\text{ Hz}$, H-5'), 7.02 (d, 1H, $J = 2.3\text{ Hz}$, H-2'), 7.13 (dd, 1H, $J = 8.0, 7.1\text{ Hz}$, H-6'), 7.33 (d, 1H, $J = 8.2\text{ Hz}$, H-7'), 7.38 (d, 1H, $J = 8.0\text{ Hz}$, H-4'), 7.50 (dd, 1H, $J = 8.1, 6.7\text{ Hz}$, H-8), 7.73 (d, 1H, $J = 7.9\text{ Hz}$, H-10), 7.80 (dd, 1H, $J = 8.3, 6.8\text{ Hz}$, H-9), 8.15 (wide s, 1H, NH-1'), 8.25 (d, 1H, $J = 6.9\text{ Hz}$, H-7); $^{13}\text{C NMR}$ (CDCl_3) δ 18.2 ($\text{CH}_3\text{-4}$), 31.6 (CH_2), 33.8 (CH_3N), 52.3 (C-4), 64.2 (C-1), 109.6 (C-3'), 111.4 (C-7'), 118.4 (C-4'), 120.2 (C-5'), 120.3 (C-6a), 122.6 (C-6'), 123.5 (C-2'), 126.8 (C-7), 127.0 (C-10), 127.1 (C-8), 127.2 (C-3a'), 134.7 (C-9), 136.0 (C-7a'), 147.5 (C-10a), 151.0 (C-11a), 160.0 (C-6), 167.2 (C-3). Anal. Calcd for $\text{C}_{22}\text{H}_{20}\text{N}_4\text{O}_2$: C, 70.97; H, 5.38; N, 15.05. Found: C, 71.10; H, 5.49; N, 15.11.

Acknowledgment. Financial support from CICYT (SAF 97-0143 and SAF-2000-0130) and the National Foundation for Cancer Research is gratefully acknowledged.

Supporting Information Available: Cartesian coordinates, energies and first normal mode for the stationary point structures and X-ray crystallographic data for **3** (1,4-anti isomer). This material is available free of charge via the Internet at <http://pubs.acs.org>.

JO015713U